China Geology 7 (2024) 63−79

China Geology

Journal homepage: http://chinageology.cgs.cn
https://www.sciencedirect.com/journal/china-geology

Age and geochemical evolution of granite magmatism in Olkhon region from Caledonian syncollisional ore-free granite to the rare metal granite and pegmatite of Middle Paleozoic intraplate setting

Viktor Antipin, Valentina Makrygina*, Larisa Kushch*, Nataliya Sheptyakova

Vinogradov Institute of Geochemistry, SB RAS, 664033 *Irkutsk, Russia*

ARTICLE INFO

Article history:
Received 18 November 2022
Received in revised form 6 July 2023
Accepted 11 July 2023
Available online 14 August 2023

Keywords:
Pegmatite
Geochemistry
Submantle plume
Magmatism
Caledonian collision
Middle Paleozoic intraplate setting
Be-Rb-Nb-Ta-Li-F mineralization
Olkhon region
Russia

ABSTRACT

The detailed description of two granite complexes in the Olkhon subterrane is given. The Early Paleozoic Sharanur complex was formed by granitization of gneisses of the Olkhon series. It includes migmatites, granite-gneisses, granites and pegmatites of normal alkalinity; they belong to the type of syncollisional granites. The Middle Paleozoic Aya granite complex includes mother Aya massif of amazonite-bearing granites and several types of rare-metal pegmatites. They have elevated alkalinity, low of Ba, Sr, and high LILE and HFSE elements contents. The Aya pegmatites lie in northwest cracks of stretching and associated with the rise of the territory under the influence of the North Asian plume. These cracks and pegmatites mark the beginning of a new intraplate geodynamic setting. Two geochemical types are distinguished among the pegmatites of this complex. These are amazonite pegmatites of Li-F type with Ta mineralization and complex type pegmatite with Be-Rb-Nb-Ta and Li-F mineralization (the Ilixin vein). The Tashkiney pegmatite vein is similar to Ilixin, but lies in the gneisses of the Olkhon series. It shows high concentrations of Be, Nb, Ta, as well as W, Sn, but lacks Li and F, due to a greater depth and higher temperature of the melt crystallization of this pegmatite.

1. Introduction

The concept of the Olkhon region for the Western Baikal area was introduced by V.S. Fedorovsky. It included Priolkhonye and Olkhon Island (Fig. 1). This region belongs to the Olkhon-Khamardaban terrane, which is part of the Central Asian Orogenic Belt (CAOB) (Windley BF, et al., 2007; Xiao W and Santosh M, 2014). Olkhon region has been studied by geologists for more than a hundred years due to its accessibility and good outcrops. From the standpoint of structural geology, part of this region is the Priolkhonye, studied by V.S.Fedorovsky on a scale of almost 1∶5000 with the involvement of aerial photographs and multi-scale satellite images, so to date there is a sound structural and geological basis for this part (Fedorovsky VS et al.,1993, 1995, 2010). But due to the complexity of its structure and the repeated tectonic rearrangements, it still contains many unresolved geological and geodynamic problems. Many unsolved problems are related to the fact that the isotope-geochemical data of geological units are scarce. Namely, they reveal in more detail the features in the development of metamorphic strata of the region and its magmatism. Recently, a wealth of data has been obtained on the absolute age of predominantly magmatic formations (U-Pb, Ar-Ar, to a lesser extent Rb-Sr, Nd-Sm methods) and significantly fewer definitions of model ages (Yudin DS et al., 2005; Vladimirov AG et al., 2008; Volkova NI et al., 2009; Gladkochub DP et al., 2010; Donskaya TV et al., 2013; Makrygina VA et al., 2010, 2014; Mikheev EI et al., 2017). These data finally confirmed the Caledonian age of major collision events in this region, but raised new questions concerning the reasons for the convergence of island-arc and collision events in time, the emplacement of voluminous basic, andesite, granitic and alkaline rocks over a narrow time interval. At the same time, the new data has revealed the onset of a new Middle Paleozoic intraplate stage in the geological history of the region.

In this paper, the authors explore the role of the protolith

First author: *E-mail address*: vant@igc.irk.ru (Antipin Viktor).

* Corresponding author: *E-mail address*: vmakr@igc.irk.ru (Makrygina Valentina); k27l27v27@ya.ru (Kushch Larisa).

Literary editor: Xi-jie Chen
doi:10.31035/cg2023040
2096-5192/© 2024 China Geology Editorial Office.

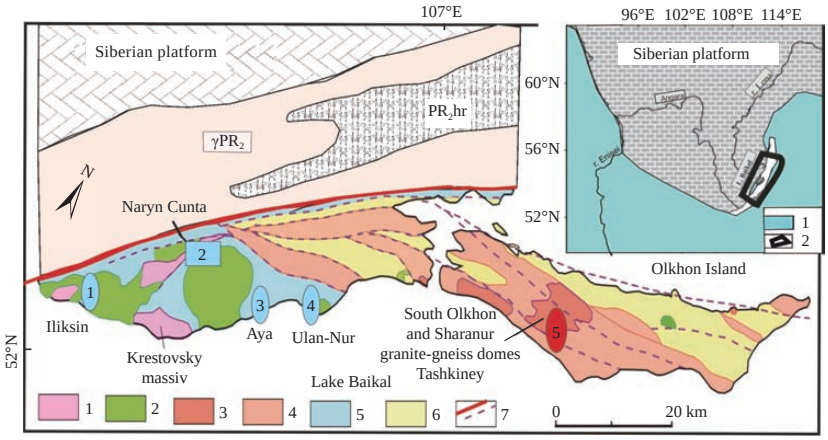

Fig. 1. Geological map of the Olkhon region (Fedorovsky, 2004, with additions by the authors). 1–gabbro, diorites, granodiorite, Khaidai complex; 2–gabbro, Ozersky complex; 3– granite; 4–granite-gneisses and migmatites, Sharanur complex; 5–dolomite marbles and volcano-terrigenous rocks (Anga series); 6–calcite marbles, gneisses, amphibolites, quartzites (Olkhon series); 7–shear zones. γPR_2 - porphiritic granites of the Primorsky complex, PR_2hr - Khargituisky stratum. Pegmatite dykes NNW striking: 1, Iliksin; 2–Naryn-Kunta; 3–Aya; 4–Ulan-Nur; 5–Tashkiney. The objects of the study are shown as ovals out of scale. Inset shows: 1–northern part of CAOB, *2*–the location of the Olkhon region.

composition and PT conditions of metamorphism in development of syncollisional and intraplate granite magmatism and in the formation of different pegmatite types. The major goals for this study are: to generalize previously obtained analytical data; to obtain more accurate data using new methods (XRD, ICP-MS); to determine the composition of rock-forming and rare minerals using the Geol Superprobe-733 and JXA 8200 microprobes.

2. Analytical methods

The authors sampled different types of pegmatites in the Priolkhonye and on the Olkhon Island. Samples of pegmatites weighing 20-70 kg were taken from fine-medium-grained zones. The study was in particular focused on rare-metal rocks of the Olkhon region, for which there were no previous accurate geochemical data. The results obtained were compared with the data of the granites from the reference Sharanur and Aya complexes. A composite analysis of fresh solid rock samples from pegmatite and granite for rare metals was performed; the samples were treated to remove weathered surfaces, cleaned with deionized water, crushed in a steel crusher, and then, crushed to <200 mesh using an agate mill. Silicate analyses were conducted according to the classical chemical method (analysts G.A. Pogudina, T.V. Ozhogina) and X-ray fluorescence (XFA) spectrometry (Amosova AA et al., 2015) according to the standard method with an error of 0.5%–5.0%.The alkaline elements were determined by flame photometry with an error of 5%–10% by L.V. Altukhova and I.M. Khmelevskaya. The concentrations of rare and rare earth elements (REE) were determined using a combined method of Inductively coupled plasma mass spectrometry (ICP-MS) and Inductively coupled plasma atomic emission spectrometry (ICP-AES) (σ ± 5%–10%) by L.A. Chuvashova and O.V. Zarubina with an error of 10%–20%. All analyses were accomplished in the Resource Sharing Center of ISC SB RAS using the equipment of the Research Scientific Center of the Institute of Geochemistry SB RAS and certified standards (Geostandards, 1994).

U-Pb zircon dating by Laser ablation and sector-field mass spectrometry with Inductively coupled plasma LA-SF-ICP-MS method was applied using a Thermo Scientific element XR single-collector SF ICP mass spectrometer at the Geological Institute, Ulan-Ude, Russia,. Measurements for standard zircons showed the error of dating less than 2%. The zircons from pegmatites of the Olkhon region was analyzed by V.B. Khubanov (Khubanov VB et al., 2016)

3. Geological divisions and metamorphism

As shown by the latest investigations based on plate tectonics theory, major structures of the Olkhon region were formed during the Caledonian collision of Olkhon terrane with the Siberian craton (Fedorovsky VS et al., 2010, 2020; Yarmolyuk VV et al., 2000; Gladkochub DP et al., 2010). The Olkhon terrane is the northern part of the Central Asian Orogenic Belt (CAOB) (Fig. 1). The Collision of the Olkhon terrane with the Siberian craton 500-480 Ma ago led to the formation of a series of thrusts in the strata of the terrane. As a result, the Olkhon and Anga strata experienced strong heating, which led to the zonal metamorphism from the granulite facies near the collision seam in the northwest to the amphibolite one in the southeast. In the rocks of the craton, weak changes are observed only in the cover, likely due to its almost vertical subsidence at the craton boundary with the terrane (Mordvinova VV et al., 2016). At the late collisional stage, the structures of the terrane rocks are complicated by a series of shifts, which were produced owing to the clockwise rotation of the craton. As evident from the thin sections, this stage is related to the repeated metamorphism with the amphibolite and epidote-amphibolite facies, superimposed on granulite and amphibolite ones, respectively (475 Ma). V.S.Fedorovsky mapped these structures on a large scale, up to 1：5000 (Fedorovsky VS et al., 1995).

The development of a series of shifts at a late collision stage led to the repited rock packs of similar compositions.

Considering this, V.S. Fedorovsky showed that instead of numerous stratigraphic sub-units revealed in the Olkhon region by previous studies, there are actually only two units - Olkhon and Anga sequences. Our geochemical studies of metasedimentary and metavolcanic rocks composition in the Olkhon area confirmed the above conclusion: there are distinctly recognizable Olkhon and Anga sequences (Fig. 1) (Makrygina VA, 2021)

The Olkhon series represents several stacked thrust sheets, a repeated series of gneiss and migmatite zones, or rather granite-gneiss domes with amphibolite margins, and interbedded members of graphite quartzites, marbles, and diopside schists (metatuffites) (Fig. 1). The predominant strike of rocks in the Olkhon series is north-eastern. The study of the Nd-Sm isotope system showed that model ageofmetasedimentary rocks is estimated at 1549–1369 Ma, consequently the sedimentary material was drifted from the fold belt (Makrygina VA et al., 2010).The metasedimentary rocks, judging by their compositions, bear evidence of destroyed older immature island arcs, reconstructed by metabasalts as EMORB. Specifically, elemental geochemistry of metasedimentary rocks indicates that their deposition occurred in a shallow, brakish (low concentrations of Li, B, F) back-arc basin under reduced conditions. The last caused the enrichment of metagraywackes, quartzites, and marbles with graphite, Cr, V, Mo, Zn, and even Ag (Makrygina VA and Antipin VS, 2018), and made this strata similar to black shales.

The 624 Ma age of two-pyroxene orthogneiss from the Chernorud zone is assumed to be very similar to the ages that constrain mafic volcanism in the Olkhon series (Volkova NI et al., 2009). Judging by concordant bedding of two-pyroxene gneisses and metasediments, this age may be interpreted as the age of sediments deposition.

The Anga series consists of basic and andesitic metavolcanics alternating with dolomitic marbles, schists and spessartine quartzites, with Mn contents up to gonditic compositions. Island-arc volcanism ended in outpourings of alkali basalts accompanied by weathering crust (Makrygina VA and Koneva AA, 2010). Thus, it is a typical complex of the mature Anga-Talanchan island arc, which continues on the eastern shore of Lake Baikal. Abundant magnetite and elevated Mn, P, and Ba contents evidence for deposition of the sediments under oxidized conditions and volcanism on the aerated slopes of the island arc. The rocks of the Anga series have experienced the accretion stage and have complex structures with varying strikes of layers. In general, they have a more basic composition than the rocks of the Olkhon series.

The rocks of the Olkhon and Anga series were subject to two stages of high-grade zonal metamorphism. Early sincollisional stage occurred under granulite facies condition along the contact with the collisional suture; the rest of the area was encompassed by the amphibolite facies. That is supported by ages of metamorphic and igneous rocks falling within 500–480 Ma (Makrygina VA and Petrova ZI, 1996). The late synshearing metamorphism(470–465 Ma) originated under amphibolite facies condition in the Olkhon series and under epidote-amphibolitic facies in Anga series. (Makrygina VA et al., 2014). It is characterized by lower temperature and pressure, that is confirmed by the presence of andalusite in rare alumina shales of the Anga series.

The folding and metamorphism of the Anga series is completed by emplacement of near-surface gabbro of the Ozersky complex (500±3.4 Ma, Yudin DS et al., 2005) and the suprasubductional gabbro-diorite-granodiorite of the Krestovsky massif of the Khaidai complex (493±3.5–477±3 Ma, Makrylina VA, Antipin VS, 2018).

4. Sharanur complex

The Sharanur granite complex in Olkhon area was allocated by E.V. Pavlovsky and A.S. Eskin (1964). The migmatites, granite-gneisses and allochthonous pegmatites in the Olkhon series were included in this complex, but their age was considered as Archean. Main features of granites and pegmatites of the Olkhon region were discussed in numerous publications (Ivanov AN and Shmakin BM, 1980; Makrygina VA, Petrova ZI, 1996; Vladimirov AG et al., 2004; Zagorsky VE et al., 2003, Antipin VS et al., 2012, 2014; Makrygina VA et al., 2018).

Currently, it is established that the Sharanur granites were produced at an age interval of 505–476 Ma during the Caledonian collision (Makrygina VA et al., 2014). Older ages were recorded in the cores of zircons, while the rims yielded younger ones. Two stages of zircon growth are consistent with two metamorphism episodes. First stage coincides with the age of the formation of thrusts. In the granulite zone, it was accompanied by enderbitization, and in the amphibolite zone by plagiomigmatization. Banded migmatites were produced in the process of metamorphic differentiation by dissolution and redeposition of quartz and plagioclase into zones of lower pressure (Fig. 2a). In general, this process is isochemical for the rock (Makrygina VA et al., 2015).

The next stage of metamorphism occurred at the late collision stage (475–465 Ma) during the transition to shear tectogenesis. Intensive K-feldspar metasomatic migmatization was maintained by increasing permeability of the sequence. It led to the growth of granite-gneiss domes (Fig. 2b), and the appearance of granite smelting with formation of biotite- and biotite-amphibole granites (Fig. 2c). The evolution of granitic melts was terminated by the production of coarse-grained quartz-feldspar pegmatites occurring near the contacts with domes and within the metamorphic sequence. The granitization didn't take place in the Anga series, due to a lower degree metamorphism on the second stage.

Our study is focused on the largest granite-gneiss domes on the Olkhon Island, Sharanur, and South Olkhon domes. They are characterized by gradual transitions from migmatites to granite-gneisses, with the melting of biotite, amphibole-biotite granites, and leucogranites in the central part of domes (Fig. 2c). The Sharanur biotite granites are composed of albite-oligoclase, K-feldspar, biotite or amphibole, and quartz,

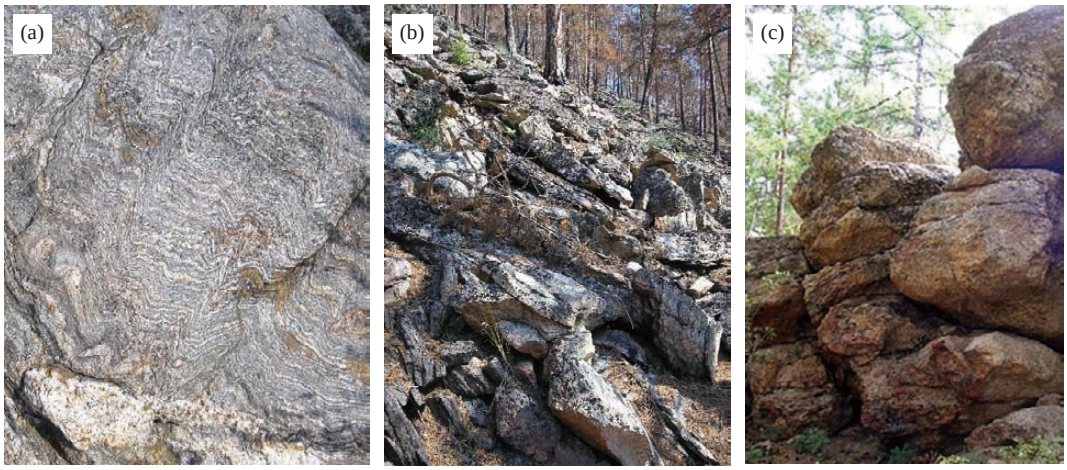

Fig. 2. The outcrops photo of migmatite (a), granite-gneisse (b) and melted biotite granite (c) of the Sharanur granite-gneisses dome near Lake Sharanur on the Olkhon Island.

and less common garnet, apatite, zircon, titanite, and allanite occurring as accessory minerals. Biotite granite falls in the field of granitic rocks of normal alkalinity, with a predominance of K over Na and ASI = 1.4–1.5 (Table 1; Fig. 3). The compositions of pegmatite veins and schlieren are similar to those of fine-grained Sharanur leucogranites and fall within series of normal alkalinity. In their trace element distribution patterns, all granite-gneisses, granites, and pegmatites are geochemically similar to them (Table 1) and represent consecutive products of the evolution of the Sharanur complex. On the spider diagrams and REE distribution diagrams, the average compositions of the schlieren pegmatites exhibit the overlap with those of the Sharanur granites (Table 1; Fig. 3; see Fig.12). All granites of the Sharanur complex demonstrate very high Ba (1000-3000 ppm) and Sr (200-400 ppm) concentrations, elevated Zr and LREE contents but very low levels of Li, Rb, Nb and other rare elements that reflect the features of the composition of the host gneiss rocks.

5. Aya rare metal granite and pegmatite complex

5.1. Aya granite massif

The Aya granite massif lies between the mouth of the Anga River and Aya Bay (Fig 1). The massif occupies an area of about 2 km^2 and is spatially confined to a large northeast-trending faulted structure composed of dolomite and calcite marbles of Anga series and lies in 500 m from the south-eastern contact of the Birkhin gabbro massif (Fig. 4). The age estimates for Aya granites vary widely from 440 to 390 Ma. Consequently, the Aya massif was intruded almost 80 Ma after the main stage of the collision. The Aya granite massif is composed of three intrusive phases: coarse-grained biotite granite, medium and fine-grained leucogranites, and the granite and pegmatite dykes (Fig. 5). The ratios of feldspars vary from phase to phase. Garnet and magnetite are present in granites of the second and third phases instead of biotite. As accessory minerals they contain apatite, zircon, and quite often fluorite (Fig. 4d). Geochemically, the later phase Aya granites are different from Sharanur granites by increased alkalinity, very low concentrations of Ba (30–215 ppm) and Sr (6–65 ppm) but elevated contents of Li, Rb, Nb, and Ta (Table 2). However, the index ASI = 1.2–1.3 in them is close to that of the Sharanur granites. Schlieren-like bodies and amazonite-bearing pegmatite dykes are widespread within the massif.

5.2. Amazonite pegmatite

In the Aya intrusion, two types of amazonite-bearing pegmatites were distinguished on the basis of vein morphology, textural relationships, and degree of the pegmatite-forming melt differentiation (Vladimirov AG et al., 2008). The first type includes lens-like or schlieren-like bodies that are generally not longer than 5–7 m, dominated by an uneven grain-size, and a graphic texture. The endocontact part of the dyke is composed of medium-grained microcline-rich granite. The second type pegmatites have a complex morphology and are generally up to 30–40 m long, with a thickness of 3–4 m. These are the most differentiated pegmatites. These dykes commonly contain white microcline and oligoclase (An - 25–30) dominated in the endocontact zones. The proportion of microcline increases towards central parts of pegmatites, which contain amazonite in association with albite (An - 4–11). Amazonite crystals up to 10–15 cm in size are found in nests.

These amazonite-bearing pegmatites contain agglomerates of zinnwaldite flakes (in some cases, in intergrowths with the garnet (up to 86 mol% of spessartine component), magnetite, and less common, muscovite and fluorite. V.B. Savelyeva (Savelyeva VB et al., 2013) revealed that the amazonite-bearing Aya pegmatite hosts Ta mineralization, represented by microlite and minerals of the columbite-tantalite series. Higher Ta concentrations are also characteristic of a number of other minerals (fergusonite, samarskite, and wolframite) from amazonite pegmatite, which also contains ixiolite, cassiterite, and zircon. Minerals that concentrate HREE elements and yttrium in the pegmatite include fluorite, monazite, xenotime, and fluorocarbonates. In combination

Table 1. Chemical composition of the biotite granite, granosyenite (PO1251), leucogranite and pegmatites of the Sharanur complex.

Component	K-Granite	Gr-Syenite		Leucogranite	Pegmatite Shlieres		
	n=7	PO1251	Shrn-70	Shrn-80	Shrn-81	Shrn-163	Shrn-177
wt.%							
SiO_2	75.45	68.49	73.94	75.70	75.20	75.00	76.00
TiO_2	0.13	0.18	0.07	0.11	0.07	0.05	0.11
Al_2O_3	13.38	16.17	14.00	13.70	14.00	13.00	12.60
Fe_2O_3	0.70	1.04	0.38	0.55	0.54	0.60	0.81
FeO	0.62	1.14	0.42	0.23	0.28	0.31	0.88
MnO	0.05	0.03	0.03	0.02	0.03	0.03	0.11
MgO	0.26	0.5	0.13	0.08	0.08	0.05	0.18
CaO	0.48	1.94	0.50	0.17	0.32	0.40	0.84
Na_2O	2.98	4.07	3.11	3.13	3.13	3.06	3.70
K_2O	5.51	4.03	6.02	5.92	6.02	6.67	3.80
P_2O_5	0.04	0.08	0.02	0.02	0.02	0.02	0.02
LOI	0.43	2.11	0.44	0.54	0.50	0.20	0.48
Total	99.99	99.71	99.13	100.10	100.06	100.05	100.03
ppm							
Li	5.9	15	5.00	4.00	5.00	2.00	2.00
Rb	137	73	196	134	140	164	62.0
Cs	<2	<2	<2	<2	<2	<2	<2
Ba	1982	2900	480	610	400	214	768
Sr	279	1300	144	216	211	101	115
Pb	35	20	39.0	34.0	33.0	45.0	25.0
Zn	49	29	26.0	28.0	29.0	10.0	22.0
Be	1.9	0.6	2.54	1.25	0.90	1.00	1.27
Sn	1.9	0.9	0.51	0.30	0.36	0.60	0.57
Cu	7	9.4	14.0	19.0	13.0	7.40	13.0
Co	1.8	6.3	1.03	0.67	1.25	0.86	1.40
Ni	13.5	13	3.32	3.80	9.00	5.60	6.30
Cr	13.1	15	2.00	2.00	2.60	3.06	6.80
V	8.3	25	2.16	0.98	6.20	3.04	3.16
Zr	186	120	96.0	117	71.0	44.0	148
Hf	5.4	3.44	3.48	4.56	2.93	2.96	4.72
Nb	4.6	4.8	7.00	3.83	1.81	7.10	6.80
Ta	1.18	0.25	0.43	0.08	0.03	0.56	0.50
Th	23.5	17.0	47.0	15.0	7.00	25.0	8.30
U	7.3	1.12	13.7	4.01	2.07	3.30	2.74
F	300	200	400	200	200	200	200
Y	26.4	0.3	4.38	1.95	2.14	27.0	15.0
La	47.5	27	11.4	7.00	8.00	8.10	8.20
Ce	109	55	20.0	32.0	14.9	20.0	19.0
Pr	9.1	5.1	1.99	1.67	1.67	2.75	2.35
Nd	31.34	22	6.95	6.00	6.00	12.1	9.30
Sm	4.77	2.3	1.20	1.09	0.92	3.90	1.62
Eu	0.65	0.70	0.54	0.41	0.63	0.20	0.57
Gd	4.90	2.30	1.12	0.84	0.77	4.80	1.90
Tb	0.79	0.24	0.15	0.11	0.08	0.90	0.34
Dy	4.98	1.06	0.84	0.50	0.44	6.40	2.91
Ho	1.10	0.16	0.18	0.09	0.09	1.41	0.86
Er	3.78	0.42	0.55	0.33	0.36	4.52	3.41
Tm	0.64	0.04	0.08	0.05	0.04	0.69	0.65
Yb	4.97	0.31	0.57	0.38	0.30	4.80	5.60
Lu	0.83	0.06	0.09	0.07	0.05	0.76	1.01
REE	225	124.7	45.67	50.5	34.2	71.3	57.7
ASI	1.49	1.61	1.44	1.45	1.49	1.28	1.51

Note: ASI = Al_2O_3/(K2O+Na_2O+CaO) (Chappell BW and White AJR, 2001).

with data from previous studies (Savelyeva VB et al., 2013), our results suggest that late amazonitic pegmatite veins, which cut the Aya granite intrusion, contain diverse rare metal minerals which allow us to classify the pegmatites as rare

metal formation having complex mineralization (Table 3).

5.3. Ulan-Nur and Naryn-Kunta pegmatites

The amazonite-bearing pegmatites lie among the Anga series rocks on the Ulan-Nur cape to the east of Aya granite massif. They form steeply dipping subparallel bodies with submeridional strike between dolomitic marbles and alkaline rocks of the Tazheran intrusive complex (Fig. 1) and stretch out over a distance of up to 1 km (Shmakin BM et al., 1973). The largest dyke among the Ulan-Nur pegmatite extends over a distance of 140 m. The dyke is composed of quartz, microcline-pertite, albite-oligoclase, and biotite. The graphic pegmatite is replaced by a zone containing large amazonite crystals, along with albite and quartz lamellaein the central part of the dyke. The graphic pegmatite of the dykes part contains sparse crystals of hornblende, garnet, tourmaline, and magnetite; biotite and muscovite may also occur in the pegmatite. Other minor and accessory minerals identified in the dyke include zircon, allanite, titanite, uranium pyrochlore, apatite, rutile, beryl, monazite, bismutite, fluorite, and molybdenite.

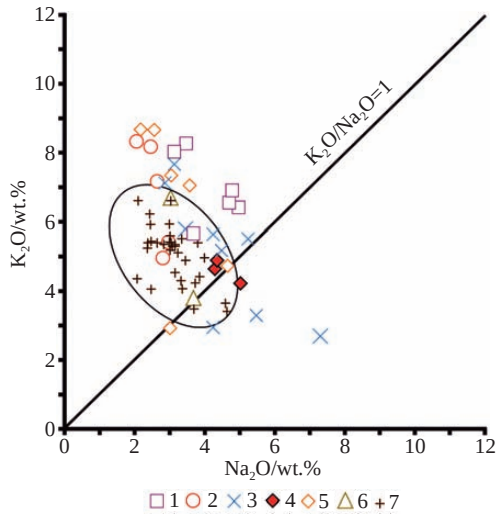

Fig. 3. K_2O *vs.* Na_2O for the Sharanur and Anga complex granitic rocks and pegmatites of various types in the Olkhon region. 1–rare metal pegmatites with Be-mineralization, Tashkiney vein; 2–Iliksin pegmatites; 3–Aya granites and pegmatites; 4– Naryn-Kunta; 5–Ulan-Nur pegmatites; 6–schlieren pegmatites of the Sharanur complex; 7–K-granites and leucogranites of the Sharanur complex (highlighted by an oval).

The studies of the Ulan-Nur rare-metal amazonite-bearing pegmatite reveal the influence of host alkaline rocks on its mineral composition. These are distinctive mineral associations containing pyrochlore, metamict zircon, fergusonite, thorite, cherchite (yttrium phosphate) and pyromorphite observed in the endocontact zone (Sklyarov EV et al., 2009).The Ulan-Nur pegmatites are similar to the Aya dykes, and according to our geochemical analyses, with respect to the mineral characteristics and REE distribution patterns (see Fig. 12) can be attributed to the Li-F type pegmatites (Table 4).

The largest Naryn-Kunta pegmatite body is located to the west of Aya granites inside the northern part of Birchin gabbro massif whose gabbro experienced cataclase and biotitization along the contact (Fig. 1). This body has the rectangular form in plane (300×155 m), and narrows with depth. Its marginal parts (10–25 m thick) are composed of medium-grained pegmatite with rare biotite and amphibole. Most of its central part was represented by large block of essentially K-feldspar pegmatite, but it was completely mined as a ceramic raw material. Separate microcline blocks have amazonite edges (2–4 cm) on contact with quartz, therefore, we refer this pegmatite to amazonite-bearing type. The medium-grained pegmatites in their trace element composition similar to the Aya biotite granites, discussed earlier. They are characterized by the same low concentrations of Ba, Sr, LREE, but high contents of Li, Rb and especially Pb (120–266 ppm) (Table 4).The accessory minerals are

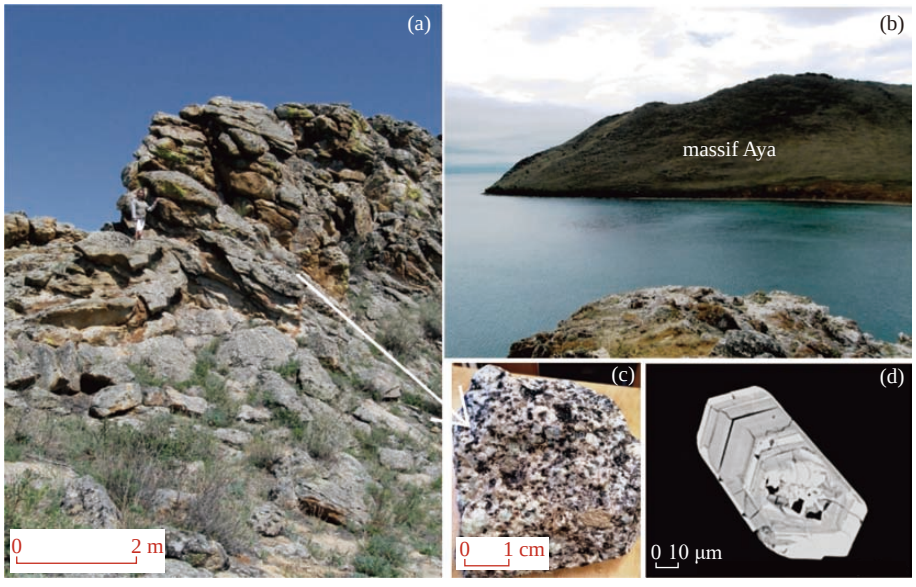

Fig. 4. Field photographs of Aya massif (b), the outcrop (a) and sample of middle-sized biotite granite (c) and back-scattered electron images of zircon (d) from Aya pegmatite.

Table 2. Chemical composition of the 1-3 phases granite and amazonite pegmatite dykes in the Aya massif.

Component	1 phase	2 phase	3 phase			Amazonite pegmatites		
	n=5	n=5	Aya589	Aya595	Aya-598	PR-621	PR-624	PR-625
wt%								
SiO_2	75.16	75.96	73.50	73.37	74.53	73.96	72.80	72.65
TiO_2	0.09	0.01	0.26	0.03	0.02	0.02	0.06	0.02
Al_2O_3	13.10	13.38	13.94	14.07	13.40	14.50	14.42	14.62
Fe_2O_3	0.55	0.34	0.70	0.43	0.34	0.21	0.17	0.08
FeO	0.93	0.41	1.47	0.77	1.18	0.44	0.64	0.96
MnO	0.02	0.03	0.03	0.03	0.12	0.05	0.04	0.25
MgO	0.10	0.03	0.34	0.02	0.03	0.05	0.05	0.05
CaO	0.60	0.19	0.80	0.18	0.52	0.16	0.06	0.74
Na_2O	4.03	4.74	4.58	3.45	5.80	4.25	3.14	4.50
K_2O	4.55	4.22	3.44	7.30	2.93	5.64	7.66	5.17
P_2O_5	0.03	0.02	0.07	0.02	0.09	0.03	0.02	0.02
LOI	0.37	0.48	0.40	0.30	0.26	0.39	0.35	0.48
Total			100.08	100.65	99.03	99.30	99.39	99.81
ppm								
Li	31	12.4	56	122	122	65.0	80.0	67.0
Rb	177	318	182	1122	1140	1105	1432	755
Cs	1	1.5	3.31	253	256	323	540	80.0
Ba	114	44	73.9	47	76.0	39.0	46.0	16.0
Sr	37	7.8	11.2	7.4	57.0	8.50	7.10	2.92
Pb	29.5	30	23	106	115	108	129	91.0
Zn	30.5	40.5	36	60	21.0	–	–	–
Be	3	3.3	3.08	13	7.20	13.6	10.8	13.0
Sn	1.59	0.75	1.35	44	1.50	32.6	43.0	15.2
Co	0.79	0.45	2.08	0.3	1.20	0.37	0.54	0.38
Ni	78	78	67	67	3.40	25.0	29.0	28.0
Cr	24.5	24	14	11.5	8.00	43.0	44.0	39.0
V	2.15	0.9	21	0.05	3.30	–	–	0.56
Y	22	22	22	99	99.0	111	99.0	249
Zr	144	119	172	54	125	121	67.0	259
Hf	4.1	6.9	4.64	5.6	5.60	12.1	7.10	23.0
Nb	10.9	55.5	15	35	113.0	35.0	36.0	98.0
Ta	0.46	4.43	1.64	28	32.0	31.0	28.0	41.0
Th	33	15.7	12.6	14.1	14.1	6.60	5.00	33.0
U	12.44	13.25	9.8	3.47	3.50	29.0	21.0	67.0
F	240	180	9.8	1100	1100	900	800	2500
Zr/Hf	35	17.2	37	9.64	22.3	10.1	9.41	11.3
Nb/Ta	23.7	12.53	9.14	1.25	3.53	1.12	1.26	2.40
Rb/Sr	3.08	40.8	16.25	151.6	20.0	129.0	201.0	258.0
Th/U	2.65	1.18	1.27	4.06	4.02	0.22	0.23	0.50
K/Rb	214	111	157	54	21.0	42.0	44.0	57.0
ASI	1.29	1.32	1.28	1.22	1.45	1.44	1.33	1.40

represented by goethite, tourmaline, zircon, and less common phenakite. Scapolite and calcite are found in endocontact zone as a result of interaction with host carbonate and basic rocks.

New U-Pb zircon ages of 443.9±2.7 Ma for the Ulan-Nur amazonite pegmatite and 440.6±2.9 Ma for Naryn-Kunta pegmatite were obtained by V.B. Khubanov using the LA-ICP-MS method (GIN SB RAS, Ulan-Ude)(Figs. 6a, b).These ages are close to each other and a little older than the age of the Aya granites and amazonite pegmatites. However, zircons from the Naryn-Kunta pegmatite had poor quality, and in single zonal grain, the core yielded the age of 470 Ma, and the rim had the age of 425 Ma. These data show a possible increase in age when using average values.

6. Rb-Nb-Ta rare-metal pegmatites

6.1. Iliksin rare-metal pegmatite dyke

The Iliksin rare-metal pegmatite dyke, lying among the Bugul'deika gabbro massif on the western part of Priolkhonye is of particular interest. Stretching along Lake Baikal, the Bugul 'deika massif located within the rocks of the Anga series and occupies an area of about 90 km^2 (Fig. 1). The pegmatite dyke extends towards north-south for about 140–145 m; its thickness varies from 50 m in the south to almost 20 m in the north. The body is crossed by a ditch, and the vertical section reveals a rather complex internal structure. The southern part includes a graphic pegmatite, composed

mainly of feldspar and quartz with biotite and garnet. In this part of the Iliksin pegmatite, no rare-metal mineralization is found. The northern part has a more dyke-like shape (Fig. 7), with protolithionite instead of biotite. In the northernmost exposure, the small block zone with albite and K-feldspar paragenesis contains the following rare-metal minerals: lepidolite, cesian beryl (vorob'evite), polychrome tourmaline, bismutho-tantalite, bismutho-columbites and fluorite (Makagon VM and Belozerova OV, 2013).

The two types of pegmatites having different mineralogy and geochemical characteristics can be distinguished in the Iliskin pegmatite body (Fig. 7; Table 5). Regarding

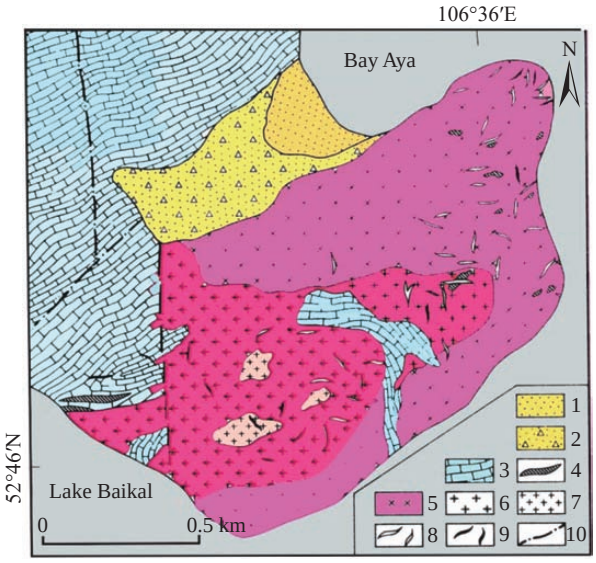

Fig. 5. Geological Map of Aya massif by (Ivanov AN, Shmakin BM, 1980) with additions by the authors. 1-2–Quaternary alluvial and deluvial deposits; 3–marble; 4–amphibolite, Anga series, PZ_2; 5–biotite granite, 1 phase; 6–granite 2 phase, with muscovite and fluorite; 7–granite 3 phase, with rare metal minerals; 8–amazonite pegmatite; 9–quartz vein; 10–faults.

Table 3. Rare earth elements in the Aya granite and pegmanite (Aya massif).

Component	Biotite granite 1 phase		2phase	3phase	F-granite	Amaz. pegm.
ppm	Aya585	Aya587	Aya578	Aya589	Aya576	Aya595
La	25	11.8	1.17	19	2.75	3.69
Ce	56	30	3.11	30	7.7	7.8
Pr	6.2	3.94	0.34	4.07	1.01	1.32
Nd	23	17	1.63	16	4.17	6.7
Sm	4.72	5.3	0.75	3.76	1.62	3.38
Eu	0.45	0.19	0.029	0.56	0.09	0.074
Gd	3.95	5.3	1.39	4.04	2.29	4.91
Tb	0.52	0.82	0.34	0.66	0.53	0.98
Dy	2.99	5.1	3.29	4.17	4.12	7.40
Ho	0.57	0.99	0.86	0.85	0.96	1.75
Er	1.71	2.93	3.62	2.69	3.53	6.90
Tm	0.25	0.43	0.67	0.41	0.60	1.39
Yb	1.64	2.75	5.6	2.72	4.77	12.9
Lu	0.25	0.41	0.91	0.40	0.70	2.20
REE	127	86.46	23.76	89.60	34.81	61.41
La/Yb	15.24	4.29	0.21	6.98	0.58	0.29

Table 4. Composition of the pegmatite Naryn-Kunta (PR-626-629) and Ulan-Nur (PR603-613).

Component	Naryn-Kunta				Ulan-Nur			
	PR-626	PR-627	PR-628	PR-629	PR-603	PR-609	PR-612	PR-613
wt%								
SiO_2	69.88	61.10	72.50	72.88	71.37	74.27	71.73	83.11
TiO_2	0.09	0.43	0.16	0.01	0.06	0.07	0.05	0.02
Al_2O_3	16.71	18.42	14.76	15.06	15.48	14.26	15.25	9.46
Fe_2O_3	0.43	1.45	0.03	0.05	0.72	0.15	0.18	0.27
FeO	0.82	3.06	0.31	0.31	0.38	0.65	0.50	0.43
MnO	0.10	0.03	0.04	0.25	0.09	0.10	0.02	0.07
MgO	0.05	0.70	0.03	0.05	0.05	0.05	0.05	0.05
CaO	1.84	5.73	0.03	0.11	0.44	0.43	0.40	0.15
Na_2O	5.52	5.36	1.96	2.45	3.05	4.66	2.57	3.02
K_2O	3.62	1.73	9.67	9.31	7.34	4.73	8.66	2.92
P_2O_5	0.03	0.02	0.07	0.02	0.02	0.02	0.02	0.02
LOI	0.39	0.36	0.35	0.48	0.36	0.25	0.22	0.11
Total	99.30	100.28	99.39	99.81	99.35	99.85	99.75	99.74
ppm								
Li	77	46	43	34	3.00	2.00	15.0	9.00
Rb	470	92	1100	2000	352	480	956	464
Cs	16.0	13.0	403	60.0				
Ba	39.0	16.0	46.0	16.0	388	70.0	70.0	7.10
Sr	8.50	6.40	7.10	2.92	133	29.0	64.0	11.5
Pb	108	72.0	129	91.0	41.0	79.0	146	88.0
Zn	–	–	–	–	77.0	39.0	32.0	41.0
Be	13.6	13.0	10.8	13.0	2.64	3.60	4.51	16.1
Sn	32.6	20.4	43.0	15.2	2.64	16.10	3.36	3.93
Cr	43.0	41.0	44.0	39.0	3.50	17.0	43.0	41.0

Table 4 (*Continued*)

Component	Naryn-Kunta					Ulan-Nur		
	PR-626	PR-627	PR-628	PR-629	PR-603	PR-609	PR-612	PR-613
V	–	–	–	0.56	9.80	2.54	3.76	0.67
Zr	121	20.0	67.0	259	81.0	25.3	12.4	11.4
Hf	12.1	1.55	7.10	23.0	6.10	3.60	1.16	3.21
Nb	35.0	99.0	36.0	98.0	27.0	52.0	17.0	17.0
Ta	31.0	21.0	28.0	41.0	3.77	10.6	8.48	5.32
Th	6.60	27.0	5.00	33.0	26.4	9.83	5.66	2.34
U	29.0	15.0	21.0	67.0	14.1	3.56	3.33	2.24
F	200	200	100	100	200	300	300	300
Y	111	19.0	99.0	249	28.0	17.5	6.10	4.91
La	0.28	5.6	0.02	0.09	2.56	4.05	0.48	0.44
Ce	0.56	16.1	0.04	0.23	6.00	9.50	1.14	1.05
Pr	0.077	2.09	0.013	0.036	0.80	1.41	0.17	0.11
Nd	0.31	9.9	0.19	0.19	3.22	6.00	0.61	0.37
Sm	0.2	5.7	0.06	0.15	1.17	2.10	0.26	0.10
Eu	0.11	0.71	0.11	0.03	0.21	0.07	0.11	0.03
Gd	0.43	10.2	0.09	0.29	2.16	2.22	0.44	0.14
Tb	0.12	2.28	0.03	0.073	0.53	0.40	0.10	0.03
Dy	0.91	17	0.19	0.52	4.30	2.31	0.74	0.27
Ho	0.22	3.83	0.05	0.11	1.04	0.42	0.20	0.07
Er	0.78	12.1	0.19	0.49	3.46	1.20	0.80	0.40
Tm	0.15	1.88	0.04	0.09	0.63	0.20	0.15	0.12
Yb	1.17	12.2	0.35	0.83	4.77	1.40	1.24	1.84
Lu	0.21	1.88	0.07	0.12	0.78	0.20	0.22	0.51
REE	5.53	101.47	1.38	3.25	31.6	31.5	6.65	5.50

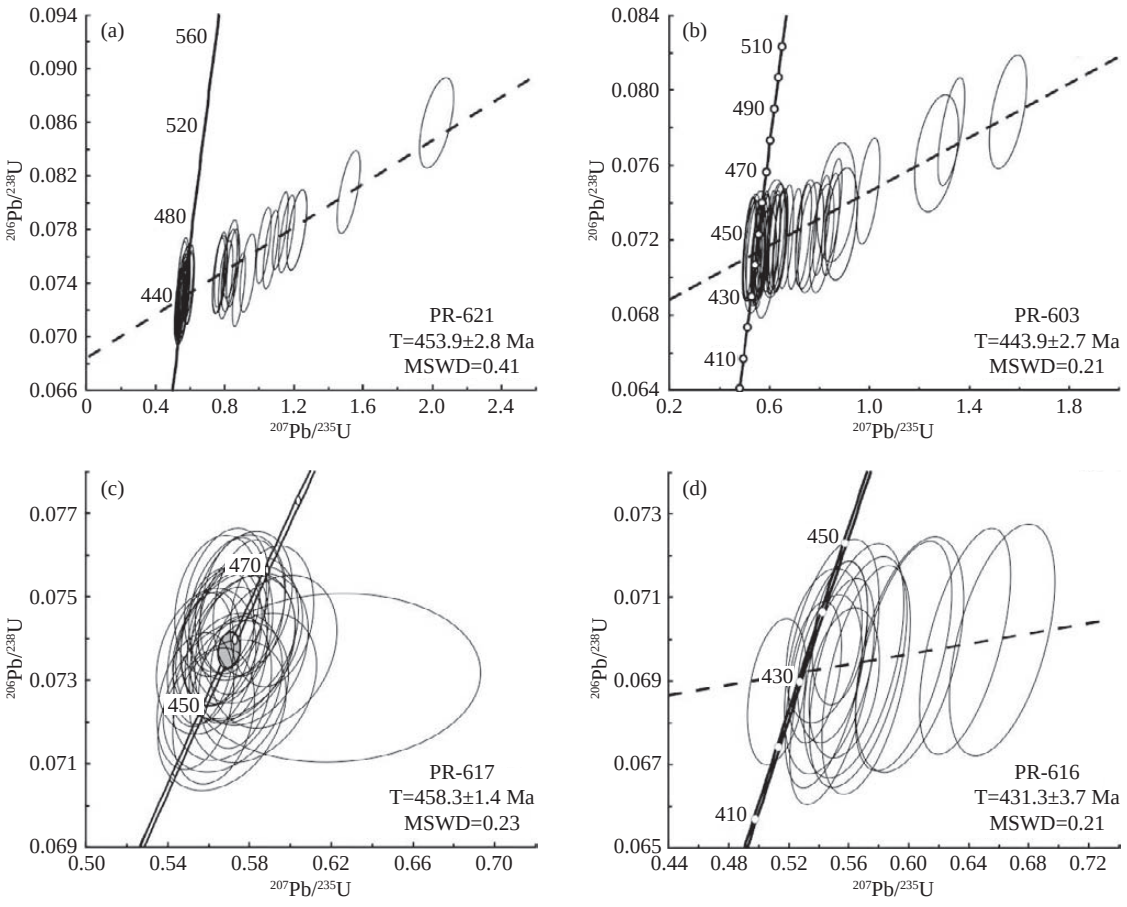

Fig. 6. Concordia diagrams for zircons from Aya amazonite pegmatites (a, b) and from the Southern Iliksin pegmatite (sample PR-617) (c) and Northern Iliksin rare-metal pegmatite (sample PR-616) (d).

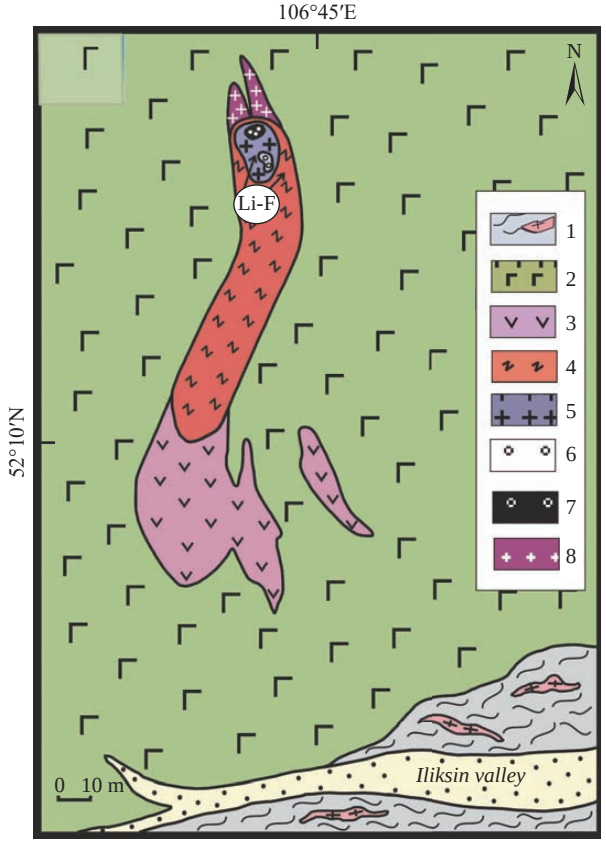

Fig. 7. Vertical section of the Iliksin pegmatite vein in gabbro of the Bugul 'deyka massif. 1–schists of Anga sequiences; 2–gabbro; 3–graphic K-feldspar pegmatite with biotite and garnet; 4–apographic pegmatite with protolithionite in middle part of the vein; 5–block of double-feldspathic pegmatite with lepidolite, tourmaline, samarskite, beryl (vorob 'evite), bismutho-tantalite, and bismutho-columbite; 6–quartz separation in the upper part of the vein; 7–inclusion of albite and fluorite; 8–quartz-albite northern end of the dyke.

K_2O/Na_2O ratio and element composition, the pegmatites from the southern part of the pegmatite(South Iliksin) are similar to the gneisses of the Olkhon series and the coarse-grained leucogranites of the Sharanur complex, lacking rare metal enrichment. The North Iliskin district hosts a typical rare-metal pegmatite of Rb-Nb-Ta type. At the same time, F-Li-Be-Ta mineralization (Li mica, fluorite, vorob 'evite, tantalite, and columbite), which characterizes this pegmatite vein as the Li-F type pegmatite, was discovered here.

The U–Pb isotope system (LA-SF-ICP-MS method) was used by V.B. Khubanov to date zircon crystals separated from different parts of the Iliksin pegmatite. The zircon from the southern graphic pegmatite yielded an age of 458 Ma (see Fig. 6c), which is well consistent with the timing of forming granites from the Sharanur dome. The zircon from the rare metal pegmatite of the northern part of the dyke (see Fig. 6d) yielded an average age of 431 Ma. This age shows that the northern rare-metal part of the dyke was produced in a submeridional crack at the post-collision stage of tectogenesis.

6.2. Tashkiney pegmatite (Olkhon Island) with Be-Nb-Ta mineralization

In the Tashkiney valley on the Olkhon Island, a zonal branched granite-pegmatite vein was discovered. This vein has submeridional striking and intersects granite-gneisses of the Sharanur dome of Olkhon series. It extends for 280 m and its thickness varies between 20 and 30 m (Fig. 8a). At its northern termination, the vein is composed of middle-grained biotite granite while its southern edge comprises apophyses of coarse–medium-grained rare-metal pegmatite (Antipin VS et al., 2014). In the southern pegmatite vein, the texture of rocks

Table 5. Chemical composition of the rare-metal pegmatites Tashkiney and Iliksin.

Component	Tashkiney				IliksinSouth		Iliksin North			
	Shrn-42	Shrn-66	Shrn-67	Shrn-136	PR-617	Bb-229	PR-616	Bb-226	Bb-222	Bb-223
wt.%										
SiO_2	68.60	72.42	70.11	71.17	72.74	74.35	77.41	74.56	–	78.11
TiO_2	0.02	0.06	0.10	0.07	0.06	0.01	0.02	0.02	–	0.01
Al_2O_3	17.20	15.10	17.10	16.30	14.50	14.00	12.30	14.40	–	13.40
Fe_2O_3	–	0.13	0.40	0.20	0.39	0.56	0.17	0.52	–	0.49
FeO	0.43	0.24	0.27	0.20	0.38	–	0.8	–	–	–
MnO	0.03	0.03	0.04	0.04	0.02	0.01	0.21	0.09	–	0.01
MgO	0.03	0.04	0.09	0.15	0.05	0.05	0.05	0.06	–	0.06
CaO	0.20	0.13	0.05	0.26	0.49	0.50	0.13	0.24	–	2.25
Na_2O	4.56	3.48	4.78	4.97	2.46	2.06	2.81	2.64	–	4.83
K_2O	8.60	8.24	6.89	6.40	8.17	8.32	4.96	7.16	–	0.52
P_2O_5	0.07	0.02	0.02	0.02	0.02	0.02	0.03	0.05	–	0.02
LOI	0.14	0.06	0.17	0.38	0.34	0.16	0.40	0.24	–	0.20
Total	100.80	100.17	100.05	99.91	99.64	99.96	99.20	100.00	–	100.01
ppm										
Li	10.0	22.0	10.0	8.00	6.00	9.00	5.00	120	88.0	195
Rb	2200	1970	1678	1747	292	752	391	4988	917	4560
Cs	140	187	279	117	8.00	14.0	8.00	620	51.0	606
Ba	20.0	82.0	77.0	37.0	323	10.7	40.0	4.57	26.0	11.0
Sr	17.0	5.70	6.70	15.0	145	87.0	16.0	5.10	7.00	27.0
Pb	113	91.0	94.0	24.0	41.0	71.0	39.0	131	95.0	30.0

Table 5 (*Continued*)

Component	Tashkiney				IliksinSouth		Iliksin North			
	Shrn-42	Shrn-66	Shrn-67	Shrn-136	PR-617	Bb-229	PR-616	Bb-226	Bb-222	Bb-223
Zn	14.6	27.0	30.0	10.0	–	5.50	24.0	46.0	32.0	5.70
Be	110	1748	316	166	0.72	1.71	2.31	176	10.8	250
Sn	51.0	40.0	63.0	31.0	0.49	0.71	13.7	5.70	13.0	0.40
W	66.0	28.0	110	65.0	–	–	–	–	–	–
Co	0.77	1.10	1.10	1.50	1.00	0.57	0.63	0.22	0.40	0.47
Ni	11.3	3.10	5.30	4.52	18.0	9.40	15.0	3.50	8.70	5.10
Cr	13.7	2.00	2.00	19.0	26.0	13.0	22.0	9.10	22.0	10.5
V	0.87	3.00	3.60	1.80	2.86	0.52	2.54	0.72	1.50	1.64
Y	96.0	60.0	73.0	127	1.89	8.50	79.0	14.4	150	25.0
Zr	26.0	25.0	22.0	41.0	20.0	6.60	12.0	11.0	158	20.0
Hf	6.40	8.00	6.40	15.0	0.89	0.58	2.32	6.10	12.5	1.50
Nb	83.0	77.0	97.0	96.0	1.68	20.0	131	105	48.0	50.0
Ta	68.0	45.0	59.0	78.0	0.13	2.41	16.0	45.0	20.0	2.60
Th	29.0	23.0	30.0	35.0	11.8	3.98	23.0	5.30	40.0	9.00
U	8.00	7.00	8.70	13.10	1.10	3.23	2.23	2.51	13.4	16.0
F	200	650	350	55.0	200	–	200	–	–	60
Y	96.0	60.0	73.0	127	1.89	8.50	79.0	14.4	150	25.0
La	21.0	4.50	25.0	24.0	2.51	1.20	16.0	2.02	7.80	0.73
Ce	65.0	13.1	65.0	83.0	6.40	1.44	47.0	3.96	16.0	1.11
Pr	9.10	2.00	8.80	12.6	0.81	0.04	6.80	0.70	2.95	0.15
Nd	36.0	8.00	33.0	52.0	3.00	0.21	27.0	3.36	14.8	0.93
Sm	16.0	4.30	13.1	25.0	0.76	0.15	12.5	1.51	7.40	0.60
Eu	0.06	0.17	0.06	0.06	0.40	0.14	0.06	0.04	0.12	0.18
Gd	12.1	3.73	9.10	18.0	0.63	0.49	9.50	1.32	9.10	1.43
Tb	1.97	0.72	1.50	2.90	0.08	0.15	1.69	0.19	1.83	0.43
Dy	9.80	3.70	70.0	13.4	0.47	1.28	11.0	0.93	12.8	3.55
Ho	1.40	0.53	0.91	1.72	0.07	0.34	2.19	0.17	3.11	0.90
Er	3.70	1.45	2.52	4.30	0.27	1.11	9.00	0.53	12.2	3.14
Tm	0.60	0.23	0.40	0.70	0.03	0.22	2.37	0.11	3.18	0.61
Yb	4.36	1.76	3.13	4.92	0.32	1.51	26.0	0.91	31.0	4.28
Lu	0.58	0.23	0.41	0.63	0.04	0.23	4.92	0.16	6.00	0.66
REE	181.7	44.4	169.9	243.2	15.8	8.50	176	16.0	128.3	18.7

changes from fine-and-medium-grained leucogranite in the endocontact zone to graphic one, with granophyric aggregates of quartz-feldspar composition in the vein center. The clusters of ruby-red garnet grains with feldspar and quartz are often associated with aggregates of beryl crystals ranging in size from 0.5–1 cm to 3–7 cm, and color varying from bluish-green to emerald-green (Fig. 8b).

The rare-metal part of pegmatite with Be-mineralization shows the following mineralogical composition: microcline (45%), plagioclase (25%), quartz (20%), biotite (2%), muscovite (5%), and beryl (3%). Zircon, magnetite, titanite, and apatite occur as accessory minerals. Monazite, zircon, xenotime, cassiterite, wolframite, thortveitite, euxenite, and a whole series of titanium-tantalum-niobates (10–25 microns in size), with admixtures of U, Th, W, Sn, and Sc, were identified in the thin sections of the rare metal Tashkiney pegmatite using the microprobe analysis (Makrygina VA et al., 2018).

We present the distribution of rare elements in the cross-section along the Tashkiney vein oriented from north to south (Table 6). The distribution pattern along the vein shows that granite in exocontact vein (Shrn-64) are similar to Sharanur granites, demonstrating high contents of Ba, Sr, and very low concentrations of Li, Rb, Cs and other rare elements. At the same time, the concentrations of Ba and Sr in the granites from the endocontact zone of the vein decrease successively, while the Rb, Cs, Be, Nb, Ta contents increase (Shrn-61). We found that increases in concentrations of these elements are particularly significant in the samples with pegmatitic texture from the southern termination. The variations in Be concentration depend on the beryl content in the sample. The Tashkiney pegmatite is depleted in Li, Ba, Sr, Eu, and Zr, but is enriched in many large-ion lithophile elements and high field strength elements (LILEs; HFSEs). Therefore, it is attributed by us to Be-Nb-Ta type of rare metal pegmatite. It is to be noted, that in contrast to Aya amazonite-bearing pegmatites, the Tashkiney pegmatite contains no amazonite. The U-Pb age of Tashkiney pegmatite zircon is 390±5 Ma (ID-TIMS, Fig. 9).

7. Discussion

As a result of previous studies of chemical composition of Sharanur and Aya granites and vein series combined with recent geochronological investigations it was inferred that Sharanur rocks were produced within the time range of

500–477 Ma, while the Aya granites formed within 440–335 Ma interval (Table 7). Such a wide age interval for Aya rocks may suggest the capture of older zircons. In such veins as Ilixin and Naryn-Kunta, the structure and mineral composition are very complex - from simple biotite varieties to rare-metal ones. Therefore, their age varies from 440 to 335 Ma, respectively.

The first interval (500–477 Ma) coincides with the timing of thrusting during the Caledonian collision of the Olkhon terrane with the Siberian Craton. The second age interval is attributed to the beginning of the Middle Paleozoic tension stage of Olkhon terrane and the transition to an intraplate geodynamic setting. The granites of Aya and amazonite and rare-metal pegmatites are characterized by an intrusive nature and placement in the northwest tension cracks. Such fracturing is most clearly visible on the satellite image of the Olkhon Island, where the Island is crossed by a series of cracks transverse to the strike of the metamorphic rocks (Fig. 10). From west to east, the 1st crack is made of medium-grained granite, the 3nd one is made of rare-metal pegmatite of Tashkiney. The rest are unfilled, but clearly visible in the relief of the Island and even in the Primorsky Ridge. These tension cracks are transverse to the syncollisional compression structures and formed 80–90 Ma after the stage of formation of the covers, that can only be explained by the transition to an intraplate geodynamic setting. This stretching can be due to the general uplift of the territory above the Middle Paleozoic North Asian plume, which caused the formation of the Angara-Vitim batholith (Yarmolyuk VV et al., 2000).

The morphological and geochemical features of granite-gneisses, granites and pegmatites of the Sharanur complex indicate their formation during granitization process of gneisses of the Olkhon series, including melting of granites.

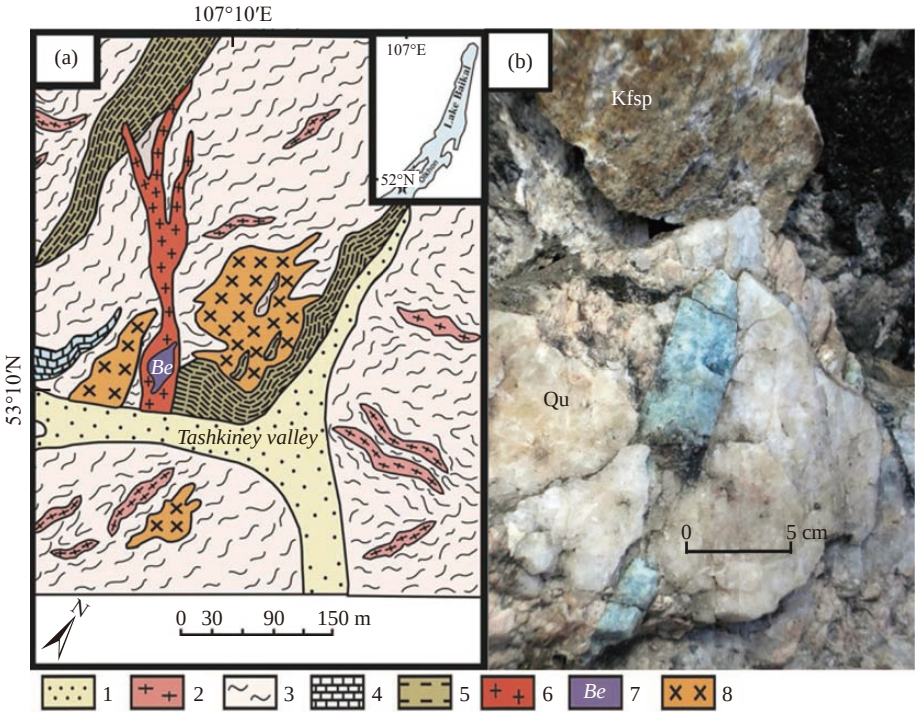

Fig. 8. A. Schematic geological structure of the Tashkiney pegmatite with Be-mineralization:. 1−Quaternary deposits; 2–granite-gneisses; 3–gneisses and migmatites. 4–marbles; 5–amphibolites; 6–rare-metal pegmatites of the vein; 7–bloky pegmatite with beryl; 8–medium-grained granosyenites, quartz syenites. B–beryl crystal in the large block feldspar-quartz zone of this vein (Photo), KFsp–K-feldspar, Qu–quartz.

Table 6. Rare metal composition of the Tashkiney pegmatite and host Sharanur granite: The cross-section along the granite-pegmatite dyke from North to South.

NN probe	Rock	Ba	Sr	Li	Rb	Cs	Be	Nb	Ta	F
Shrn-64	Granite, exocontact	2094	1249	4	56	0.8	1.5	4	1	300
Shrn-61	Granite, endocontact	239	32	3	239	2.7	4.7	55	3.6	220
Shrn-62	Medium-grained part	713	270	4	380	12.4	9.7	217	16.4	250
Shrn-65	Be-Pegmatite	737	21	24	872	240	958	145	60	370
Shrn-66	Blocky pegmatite	1008	21	6	1920	248	27	42	21	500
Shrn-67	Be-Pegmatite	82	6	22	1810	187	748	67	45	650
Shrn-68	Be-Pegmatite	77	6.7	10	1640	279	316	97	59	350
Shrn-69	BlockyPegmatite	73	14	14	1890	311	84	36	19	600
Shrn-136	Be-Pegmatite	37	15	n.anal.	1747	n.anal.	166	96	78	n.anal.
Shrn-137	Be-Pegmatite	342	16	n.anal.	1443	n.anal.	335	53	32	n.anal.

Granite-gneisses and granites inherit from host gneisses, high Al, Ba, Sr, Zr, but low Li, Rb, Cs and other rare elements concentrations. In their K_2O/Na_2O=1.0–1.5 and value $Al_2O_3/(K_2O+Na_2O+CaO)$=1.4–1.5), they can be attributed to S-type granites (Chappell BW and White AJR, 2001).

Geochemical differences of both granite complexes are in particular visible in element ratio diagrams. The of K/Rb to Rb ratio clearly shows a sharp increase in the contents of rubidium in the derivatives of the Aya granites (Fig. 11a). The analysis of K/Rb to Nb/Ta values demonstrates a clear increase in the role of tantalum in the Aya derivatives and Nb in the Sharanur ones (Fig. 11b). Finally, the derivatives of the

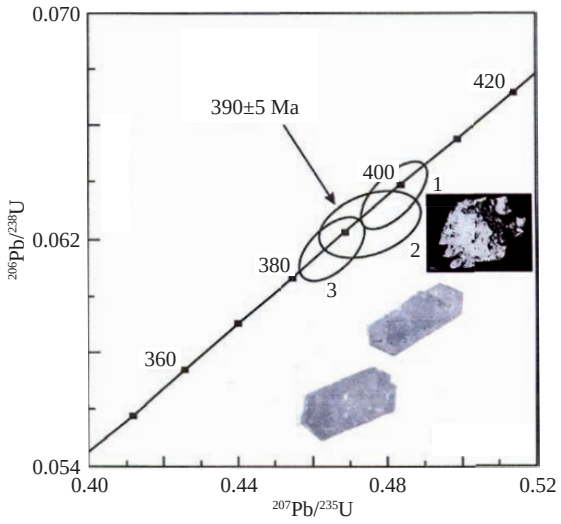

Fig. 9. U–Pb concordia diagram for zircons from the Tashkiney coarse-grained rare-metal pegmatites with Be-mineralization (sample shrn-137), U-Pb ID-TIMS method.

Aya rocks are depleted in barium and strontium (Fig. 11c). The same differences are visible on the spider diagrams of rare and rare earth elements (Figs. 12a, b).

In their rare element compositions, the derivatives of the Sharanur granites plot in Pearce diagram (Pearce JA et al., 1984; Pearce JA, 1996) close to boundary of the island arcs granites and syncollisional granites (Figs. 13a, b). Our data suggest that this is due to the fact that the gneisses protolith has an island-arc nature.

The second Aya complex of the intrusive amazonite-containing granites and rare-metal pegmatites lies in the upper lithological unit of the Anga series composing of metavolcanics, dolomitic marbles and quartzites of the epidote-amphibolite facies. The granitization is not manifested in the Anga series due to lower temperatures. The granites and series of pegmatites of the Aya complex differ from the Sharanur complex by increased alkalinity, but by a close value of the ASI criterion = 1.3–1.4. They are exceptionally poor in Ba and Sr but enriched with Rb, Nb, Ta, as well as Li, F. In these indicators, Aya granites are close to A-type granites (King PL et al., 2001). In Pearce diagrams, the intrusive derivatives of the Aya complex plot in the field of intraplate granites (Fig. 13). Pegmatites enriched in Li, Be, Rb, Cs, Nb, Ta, F can be classified as the complex Be-Nb-Ta pegmatite type containing Li and F.

In contrast to the Aya amazonite and rare-metal pegmatite, the Tashkiney pegmatite vein lies within the Sharanur granite-gneisses in the lower Olkhon sequence. However, it is submeridionally oriented and has an age of 390 Ma. The Tashkiney dyke contains no lithium and fluoride-containing minerals but a considerable amount of beryl and minerals of HFSE and LILEs. Therefore, the Tashkiney pegmatite belongs to the Be-Nb-Ta type of rare metal pegmatites. On the

Table 7. The izotope U-Pb, Ar-Ar dating of the Granite and pegmatite Ol'khon region.

Place	Rock	Mineral	Method	Age, Ma	Reference
	Sharanur complex				
South Olkhon dome	Granosyenite	Zircon	Shrimp-II	495±6	Gladkochub DP et al., 2010
South Olkhon dome	Granosyenite	Zircon	U-Pb	490	Letnikov FA et al., 1995
Sharanur dome	Bi-granite	Zircon core	Shrimp-II	505±12	Makrygina VA et al., 2014
		" rim		476±4.2	"-"
Tutai massif	Bi-Amph granite	Zircon core	Shrimp-II	488,6±8	Donskaya TV et al., 2013
		" rim	U-Pb	464±11	"-"
		Zircon core		498±4	"-"
		" rim		472±3	"-"
	Aya complex				
Aya massif	Granite	Zircon	U-Pb	410	Letnikov FA et al., 1995
Aya massif	Granite	Biotite	Ar-Ar	391.1±3.9	Yudin DS et al., 2005
Aya massif	Amaz.pegmatite	Biotite	"	412.86±4.2	"-"
Naryn-Kunta	Pegmatite med/grain	Amphibole	"	410±2	"-"
Aya massif	Amaz.pegmatite	Zircon	LA-ICP-MS	334.8±2	This paper
Naryn-Kunta	"-"	Zircon	U-Pb	440.6±2.9	"-"
"-"	"-"	Zircon core	"-"	470	"-"
"-"	"-"	" rim	"-"	425	"-"
Ulan-Nur	Amaz. Pegmatite	Zircon	"-"	443.9±2.7	"-"
Iliksin South	Bi-pegmatite	Zircon	"-"	458.3±1.4	"-"
Iliksin North	Rare metal pegmatite	Zircon	"-"	431.4±2.6	"-"
Tashkiney pegmatite	Be-pegmatite	Zircon	ID-TIMS	390±5	Makrygina VA et al., 2018

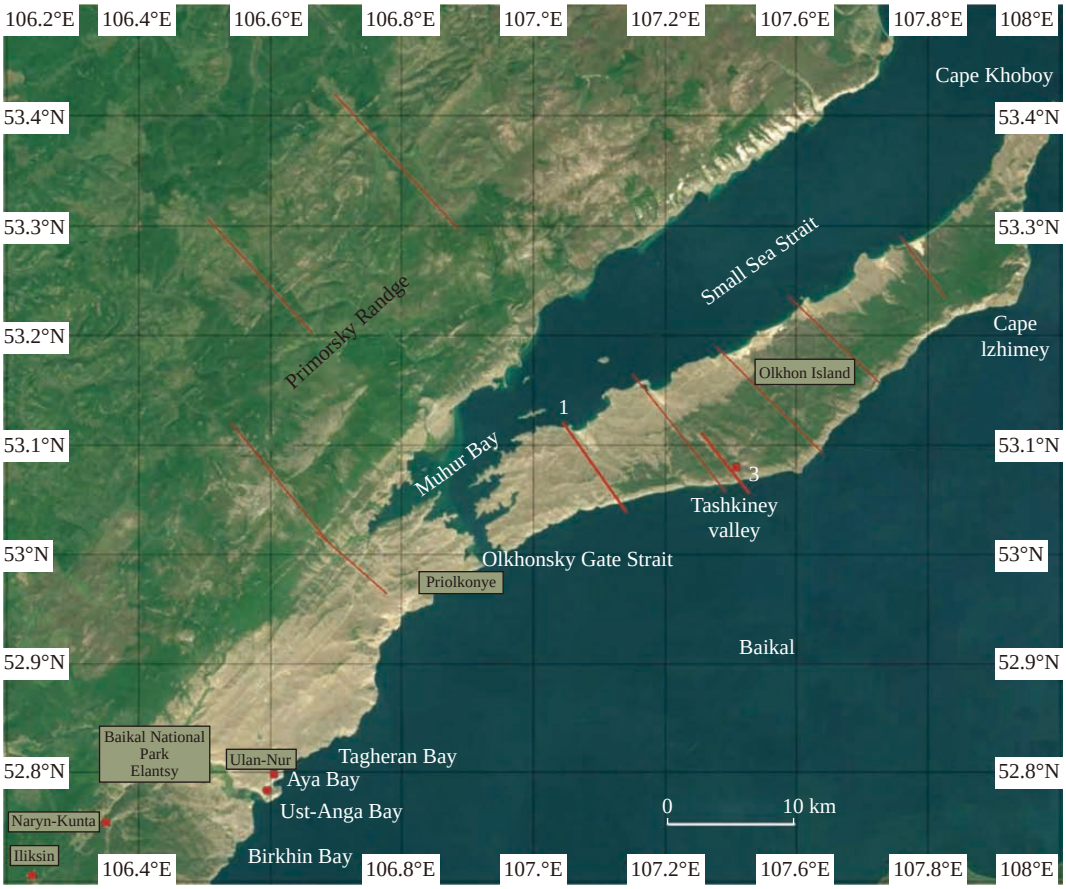

Fig. 10. A satellite image of the Olkhon region. The direction of the Middle Paleozoic fracturing is shown by red lines: from west to east, the 1st crack is made of medium-grained granite, the 3nd one is made of rare-metal pegmatite of Tashkiney.

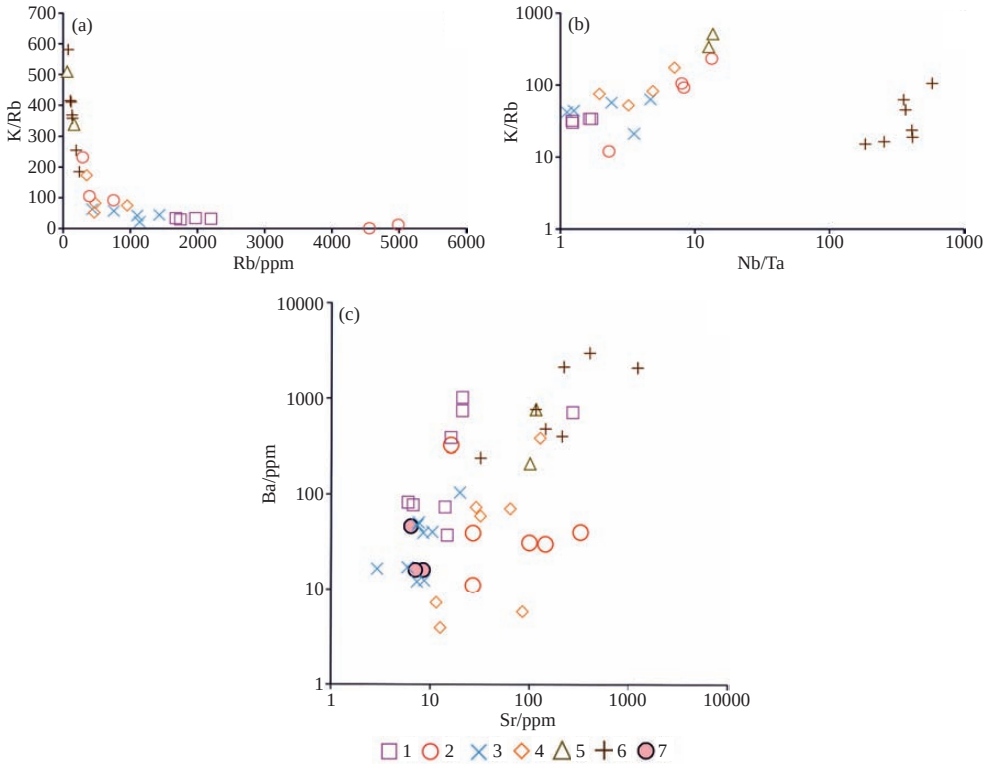

Fig. 11. Correlation diagrams of rare elements ratios in the granite and pegmatite Sharanur and Aya complexes. 1–rare metal pegmatites with Be-mineralization, Tashkiney vein; 2– Iliksin pegmatites; 3–Aya granites and pegmatites; 4–Ulan-Nur pegmatites; 5–schlieren pegmatites of the Sharanur complex; 6–K-granites and leucogranites of the Sharanur complex; 7–Naryn-Kunta.

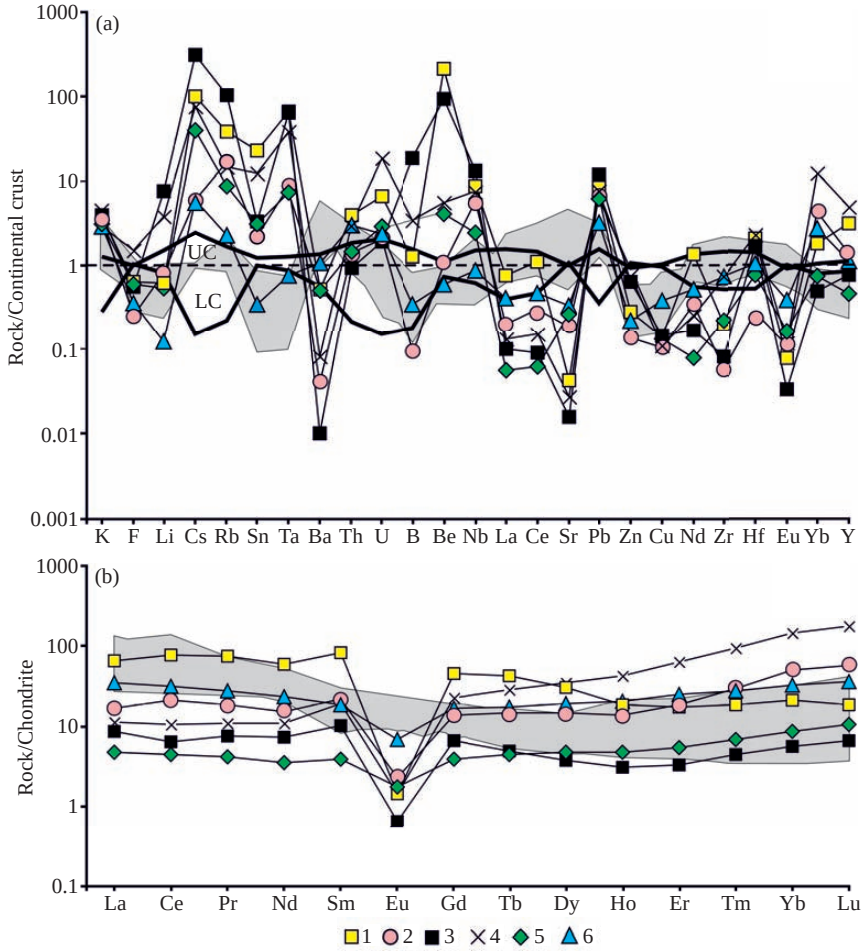

Fig. 12. Spider diagrams of the distribution of rare (a) and rare-earth elements (b) in Sharanur granitic rocks and in the Aya complex of amazonite granite and rare-metal pegmatites. 1–rare metal pegmatites with Be-mineralization, Tashkiney; 2–Southern Iliksin pegmatites; 3–Nothern Iliksin rare metal pegmatite; 4–Aya pegmatite; 5–Ulan-Nur pegmatite; 6–average composition of the Sharanur granite (grey field in the diagram). All element contents are normalized to the average composition of the continental crust (Rudnick RL et al., 2003) (Fig. 12a); LC–compositions of the lower continental crust, UC–upper continental crust. The contents of rare-earth elements (REE) (Fig. 12b) are normalized to chondrite composition (C1) (McDonough WF et al., 1995).

Pierce discrimination diagrams, the Tashkiney pegmatite like the derivatives of the Aya granites plot in the field of intraplate granites (Figs. 13a, b).

The Nd-Sr isotopic composition for the both granites complexes was determined by A.G. Vladimirov: the positive $\varepsilon_{Nd}T$ values +0.9–2.9 in the granites of the Aya complex and sharply negative ε_{Nd} T values (=−15–20) in the Sharanur granites (Vladimirov AG et al., 2008). In his viewpoint, the granites of these complexes have different sources of substances: metasomatic reworking of the continental crust substance with granite smelting during collision stage in the case of Sharanur S-granites, and acid melting from juvenile oceanic crust in the case the of the Aya granites formation.

8. Conclusions

(i) The products of two granite complexes widely occur in the Olkhon region: (1) the Early Paleozoic Sharanur S-type granite formed in the collisional setting with the age 495–480 Ma, and (2) the Middle Paleozoic Aya rare-metal granite and pegmatite (440–335 Ma), denoting the transition to an intraplate geodynamic setting.

(ii) The Sharanur migmatites, granite-gneisses, granites and schlieren pegmatites were produced in situ within the gneisses of the lower Olkhon series. The Aya granites and rare-metal pegmatites lie within the gabbro and carbonate rocks of the upper Anga series and occupy the submeridional fractures, marking the beginning of the extensional structures of a new intraplate geodynamic setting. Their Sm-Nd isotopic composition suggest the melting of the ancient oceanic crust material.

(iii) According to the age of 440–335 Ma and geographical location, as well as geochemical characteristics, the Aya granites and pegmatites may belong to the marginal part of the large Middle Paleozoic granite Angara-Vitim batholith.

(iv) Several types of rare-metal pegmatites are distinguished in the Aya complex: amazonite with Li-F and complex rare-metal mineralization, and Be-Nb-Ta rare-metal type, without amazonite.

CRediT authorship contribution statement

Viktor Antipin, Valentina Makrygina: Conceptualization.

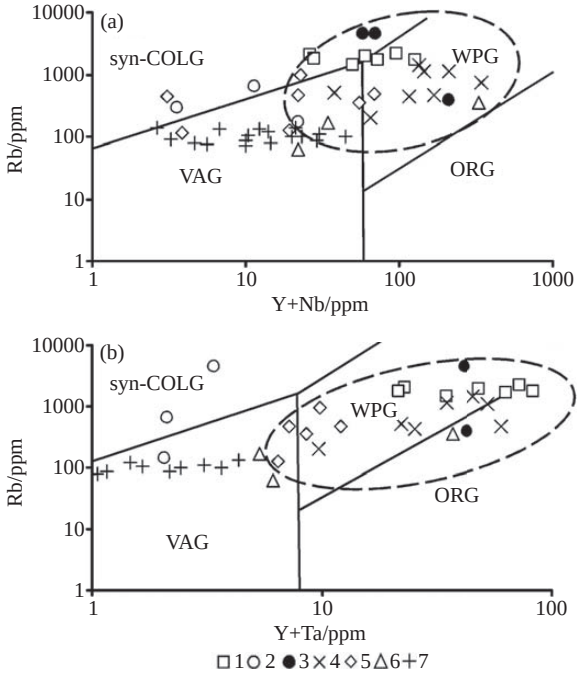

Fig. 13. Geotectonic discrimination diagrams for the granite and pegmatites of Sharanur and Aya complexes, Olkhon region: a–Rb-(Y+Nb); b–Rb-(Yb+Ta), according to Pearce J.A. (Pearce JA et al., 1984; Pearce JA, 1996). 1–rare-metal pegmatites with Be-mineralization, Tashkiney; 2–Iliksin South pegmatites; 3–Iliksin North pegmatites; 4–Aya pegmatites; 5–Ulan-Nur pegmatites; 6–schlieren pegmatites of the Sharanur complex; 7–K-granites and leucogranites, Sharanur complex. Abbreviations: syn–COLG - syncollision granites, ORG–ocean ridge granites, VAG–volcanic arc granites, WPG–intraplate granites. Fields on diagrams a and b (highlighted by an oval): rare-metal pegmatites.

Viktor Antipin, Larisa Kushch, Nataliya Sheptyakova: Methodology. Viktor Antipin, Larisa Kushch, Nataliya Sheptyakova: Validation. Nataliya Sheptyakova, Larisa Kushch: Data curation. Viktor Antipin: Original draft preparation. Viktor Antipin, Valentina Makrygina, Larisa Kushch, Nataliya Sheptyakova: Writing-review and editing. All authors have read and agreed to the published version of the manuscript.

Declaration of Competing Interest

The authors declare that they have no known competing financial interests or personal relationships that could have appeared to influence the work reported in this paper.

Acknowledgments

The authors would like to thank M. Khomutova for editing in English. We would like to thank V. Khubanov (Institute of Geology SB RAS, Ulan-Ude) for performing U-Pb dating of samples. The study was conducted within the framework of the state task (topic ID 0350-2019-0007) and supported by grant 20-55-44002-Mong_a of the Russian Foundation for Basic Research. The authors also want to thank the reviewers and editors for their contribution to improving this article.

References

Amosova AA, Panteeva SV, Tatarinov VV, Chubarov VM, Finkelshtein AL. 2015. X-ray fluorescence determination of major rock forming elements in small samples 50 and 110 mg. Anal. Contr. 19, 130–138 (In Russian).

Antipin VS, Gorlacheva NV, Makrygina VA 2014. Geochemistry of Early Paleozoic granitoids of the Baikal region and their geodynamic setting exemplified by the Khamar-Daban Ridge and Olkhon Island. Russion Geology and Geophysics. 55(2). 177–189.

Antipin VS, Gorlacheva NV, Makrygina VA, Kushch LV 2012. Composition and geochemical typization of granitoids from Olkhon Island (Sharanurskii complex). Doklady Earth Sciences. V. 445. Part 1. 858–862.

Antipin VS, Kushch LV, Sheptyakova NV, Vladimirov AG. 2018. Geochemical evolution of the early Paleozoic collisional magmatism from autochthonous migmatites and granites to multiphase granite intrusions (Sharanur and Aya complexes, Baikal Region). Russ. Geol. Geophys. 59(12). 1616–1625. doi: 10.15372/GiG20181207.

Chappell BW and White AJR 2001. Two contrasting granite types: 25 years later. Australian Journal of Earth Sciences. 48. 489–499.

Donskaya TV, Gladkochub DP, Fedorovsky VS, Mazukabzov AM, Cho, M, Cheong, W, Kim J, 2013. Synmetamorphic granites (~490 Ma) as accretion indicators in the evolution of the Olkhon terrane (western Cisbaikalia). Russ. Geol. Geophys. 54 (10), 1205–1218.

Fedorovsky VS, Dobrzhinetskaya LF, Molchanov TV, Likhachev AB, 1993. A new type of mélange (Baikal, Olkhon region). Geotectonika. No 4. 30–45.

Fedorovsky VS, Vladimirov AG, Khain EV, Kargopolov SA, Gibsher AS, Izokh AE. 1995. Tectonics, metamorphism and magmatism of collision zones of Central Asian Caledonides. Geotektonika 3, 3–22.

Fedorovsky VS, Sklyarov EV. 2010. Olkhon Geodynamic proving ground (Lake Baikal): High-resolution satellite data and a new generation geological map Geodynamics and Tectonophysics, 1(4), 331–418. doi. org/10.5800/GT-2010-1-4-0026.

Fedorovsky VS, Sklyarov EV, Gladkochub DP, Mazukabzov AM, Donskaya TV, Lavrenchuk AV, Starikova AE, Dobretsov NL, Kotov AB, Tevelev AV. 2020. Collision system of the West Baikal region: Aerospace geological map of the Olkhon region (Baikal, Russia). Geodynamics and tectonophysics, 3, URL: https://cyberleninka.ru/article/n/kollizionnaya-sistema-zapadnogo-pribaykalya-aerokosmicheskaya-geologicheskaya-karta-olhonskogo-regiona-baykal-rossiya.

Geostandards Newletter, 1994. Vol. 18. Spec. Issue, July.

Gladkochub DP, Donskaya TV, Fedorovsky VS, Mazukabzov AM, Larionov AN, Sergeev SA, 2010. The Olkhon metamorphic terrane in the Baikal region: An Early Paleozoic collage of Neoproterozoic active margin fragments. Russ. Geol. Geophys. 51(5), 447–460.

Ivanov AN, Shmakin BM. 1980. Granite and pegmatite formation of the West PreBaikalie. Moscow: 218 p. (in Russian)

Khubanov VB, Buyantuev MD, Tsygankov AA. 2016. U-Pb dating of zircons from PZ3-MZ igneous complexes of Transbaikalia by sector-field mass spectrometry with laser sampling: technique and comperison with SHRIMP. Russ. Geol. Geophys. 57(1), 241–258. doi: 10.15372/GiG20160113.

King PL Chappell BW, Allen CM & White J. R. 2001. Are A-type the high temperature felsic granites? Evidence from fractionated granites of the Wangrah Suite. Australian Journ. of Earth Sciences. 48, 501–514.

Letnikov FA, Khalilov VA, Savelyeva VB, 1995. Isotope dating of the endogenic processes in Pryolkhonie. Dokl. Earth Sci. 344 (1), 96–100.

Makagon VM, Belozerova OYu, 2013. Bismutotantalite from pegmatites of the Western Baikal Region, East Siberia, Russia. PEG, Abstracts. New Hampshire, USA, 88–89.

Makrygina VA, 2021. Specifics of Caledonian Collision in the Olkhon region (Lake Baikal, Russia). Russ. Geology and Geophysics, 62(4), 389–400.

Makrygina VA, Antipin VS, 2018. Petrology and Geochemistry of Metamorphic and Igneous Rocks of the Olkhon Region; GEO Novosibirsk, 248 p. doi: 10/21782/B978-5-9909584-4-9 . (in Russian).

Makrygina VA, Koneva AA. 2010. Geochemistry of over deposited and overdeposited wethering cores, PreBaikalie . Geochem. Int., No 8. 765–777.

Makrygina VA, Petrova ZI. 1996. Geochemistry of migmatite and granite Preolkhonie and Olkhon Island (West PreBaikalie). Geochem. Int., 34(7), .574–585.

Makrygina VA, Sandimirov IV, Sandimirova GP, Pakholchenko YuA, Kotov AB, Kovach VP, Travin AV. 2010. Nd-Sr systematiks of magmatic rocks of the Anga and Talanchanka sequences of middle Baikal. Geochem. Intern., 48(10), 979–987 . doi: 10.1134/S0016 702910100034.

Makrygina VA, Suvorova, LF, Antipin VS, Makagon VM. 2018. Rare-metal pegmatoid granites, markes of the beginning of the Hercynian within-plate stage in the Olkhon region of the Baikal area. Russ. Geol. Geophys. 59(12), 1626–1639. doi: 10.15372/GiG20181208.

Makrygina VA, Suvorova LF. Lepekhina EN. 2015. Fluid regime of the initial stages of granite formation in metamorphic complexes of different pressures. Geochem. Int. No 4. 312–326.

Makrygina VA, Tolmacheva EV, Lepekhina EN. 2014. Cristallization History of Paleozoic granitoids in the Olkhon region, Lake, Baikal (Shrimp-II zircon dating). Russ. Geology and Geophisics, 55,(1), 33–45. doi: 10.1016/j.rgg.2013.12.010.

McDonough WF, Sun S-S, 1995. The Composition of the Earth. Chemical Geology 120, 223–253. https://doi.org/10.1016/0009-2541(94)00140-4.

Mikheev EI, Vladimirov AG, Fedorovsky VS, Bayanova TB, Mazukabzov AM, Travin AV, Volkova NI, Khromykh SV, Khlestov VV, Tishin PA, 2017. Age of overthrust-type complex granites in accretionary–collisional system of the early Caledonides (western Baikal region). Dokl. Earth Sci. 472(2), 152–158. doi: 10.7868/ S0869565217050206.

Mordvinova VV, Kobelev MM, Treussov AV, Khritova MA, Trunkova DS, Kobeleva EA, Lukhneva OK. 2016. Deep structure of the Sibirian platform – Central Asian mobile belt transitions zone from teleseismic data. Geodynamics & Tectonophysics. V. 7. Iss. 1. P. 85–103.

Pavlovsky EV, Eskin AS. 1964. Composition features and structures Arkhean of PreBaikalie. /Editor V. G. Belichenko/ - M.: Science, 128 p. (In Russian).

Pearce JA, 1996. A user's guide to basalt discrimination diagrams. In: Wyman, D. A. (ed.) Trace Element Geochemistry of Volcanic Rocks: Applications for Massive Sulphide Exploration. Geological Association of Canada, Short Course Notes 12, 79–113.

Pearce JA, Harris NBW, Tindle AG. 1984. Trace element discrimination diagrams for the tectonic interpretation of granitic rocks. Journal of Petrology 25, 956–983. doi: 10.1093/petrology/25.4.956.

Rudnick RL, Gao S. 2003. Composition of the Continental Crust. In: Holland H. D, Turekian KK (eds). Treatise on Geochemistry. Elsevier-Pergamon, Oxford 3, 1–64. doi: 10.1016/B0-08-043751-6/03016-4.

Savelyeva VB, Kanakin SV, Karmanov NS. 2013. New data on mineralogy of amazonite pegmatites in Priolkhonye (Western Baikal Region). Zapisky RMO, Pt CXLII, 2, 44–66.

Shmakin BM, Makagon VM, Koneva AA, Ivanov AN. 1973. Amazonite pegmatites of the Olkhon Region (Western Baikal area). Zapisky RMO, 103, 5, 591–599. (In Russian).

Sklyarov EV, Fedorovsky VS, Kotov AB, Lavrenchuk AV, Mazukabzov AM, Levitsky VI, Sal 'nikova EB, Starikova AE, Yakovleva SZ, Anisimova IV, Fedoseenko AM, 2009. Carbonatites in collisional settings and pseudo-carbonatites of the Early Paleozoic Olkhon collisional system. Russ. Geol. Geophys. 50, 12, 1091–1106 (1405–1423).

Vladimirov AG, Khromykh SV, Fedorovsky VS, Khlestov VV, Volkova NI, Vladimirov VG, Travin AV, Yudin DS, Sergeev SA, Matukov DA. 2004. Stress granites and their significance for assessing the duration and intensity of tectonic metamorphic events during collisional orogeny Geodynamic evolution of the lithosphere of the Central Asian mobile belt (from the ocean to the continent). Materials of the scientific meeting on the Program of Fundamental research, 2, 67–71.

Vladimirov AG, Khromykh SV, Mekhonoshin AS, Volkova NI, Travin AV, Yudin DS, Kruk NN. 2008. U–Pb dating and Sm–Nd systematics of igneous rocks in the Olkhon region (Western Baikal Coast). Dokl. Earth Sci., 423(5), 651–655 . doi: 10.1134/S1028334 X08090092.

Volkova NI, Travin AV, Vladimirov AG, Mekhonoshin AS, Khromykh SV, Yudin DS, Matukov DI, Lepekhina EN. 2009. The first data on the age of the oceanic crust of the Olkhon region (according to the results of U-Pb zirconometry of granulites, SHRIMP-II. Geodynamic evolution of the lithosphere of the Central Asian mobile belt (from the ocean to the continent). Materials of the meeting, 65–67.

Windley BF, Alexeiev D, Xiao W, Kröner A, Badarch G. 2007. Tectonic models for accretion of the Central Asian Orogenic Belt. J Geol Soc. London, 164, 31–47. doi: 10.1144/0016-76492006-022.

Xiao W, Santosh M. 2014, The western Central Asian Orogenic Belt: A window to accretionary orogenesis and continental growth: Gondwana Research, v. 25, pp. 1429–1444.

Yarmolyuk VV, Kovalenko VI, Kuzmin MI. 2000. North-Asian activity superplume in the Phanerozoic: magmatism and geodynamics. Geotektonika 5, 3–29.

Yudin DS, Khromykh SV, Mekhonoshin AS, Vladimirov AG, Travin AV, Kolotilina TB, Volkova MG. 2005. $^{40}Ar/^{39}$ Ar age and geochemical features of syncollisional gabbroids and granites from the Western Baikal Region: evidence from the Birkhin massif and its folded framing. Dokl. Earth Sci. 405(2), 1261–1265. Rus. 251–255.

Zagorsky VE, Makagon VM, Shmakin BM, 2003. Systematics of the granite pegmatites. Russ. Geol. Geophys. 44, 5, 422–435. doi: 10.31241/FNS.2018.15.064.